Superparamagnetism and spin-glass freezing in nickel-manganese alloys

Ronald B. Goldfarb* and Carl E. Patton

Department of Physics, Colorado State University, Fort Collins, Colorado 80523

An experimental study of the ac susceptibility, magnetization, and thermoremanent magnetization has been made for atomically disordered and weakly ordered Ni_3Mn. Superparamagnetism with cluster interaction is demonstrated by Curie-Weiss behavior above the susceptibility peak temperature and a Langevin dependence of the magnetization. Blocking is suggested by a weak frequency dependence of the susceptibility peak and an increase in hysteresis below the peak temperature. Spin freezing, which fixes the direction of the local anisotropy, is examined by thermoremanent magnetization measurements.

I. INTRODUCTION

Atomically disordered and weakly ordered nickel-manganese alloys near the Ni_3Mn composition have certain unusual magnetic properties below room temperature which can phenomenologically be described as mictomagnetic.[1] One of these properties is a unidirectional anisotropy induced by field cooling to liquid-helium temperatures which causes a shifted hysteresis loop and a thermoremanent magnetization (TRM) in the direction of the cooling field. Such displaced hysteresis loops are evidence of exchange anisotropy.[2] In disordered Ni-Mn and related alloys, the concept has been applied to ferromagnetic and antiferromagnetic domains[3] as well as interactions at the nearest-neighbor atomic level.[4] Annealing quenched Ni_3Mn at 500 °C for brief periods of time increases the degree of short-range atomic order.[5] One of the consequences of this weak ordering is a 180° reversal in thermoremanent magnetization upon warming, after prior field cooling to liquid-helium temperatures.[6]

The early work on Ni-Mn by Kouvel *et al.* establishes the alloy as the first in which mictomagnetic or spin-glass properties were observed.[2] Since then, however, emphasis has been on somewhat simpler systems of dilute magnetic constituents in nonmagnetic hosts. Specific work has focused primarily on the intriguing sharp cusp in susceptibility at low temperature, not accompanied by any classical phase transition. Little attention has been given to the broad peaks in susceptibility seen in more concentrated alloys, particulary those composed entirely of magnetic elements, such as Ni-Mn. Wohlfarth has pointed out that such peaks are often seen in rock magnetism.[7] Furthermore, there is a well established connection in rock magnetism between thermoremanent magnetization effects, such as those seen in mictomagnets, and superparamagnetism.

The objective of the present study was to examine the various magnetic properties of Ni_3Mn below room temperature and to elucidate the magnetic ordering processes which lead to the susceptibility behavior and the thermoremanent properties alluded to above. Included were measurements of low-field ac susceptibility versus temperature, magnetization versus temperature, hysteresis, thermoremanent magnetization (TRM) after field cooling from 300 to 4 K, and partial thermoremanent magnetization (PTRM) after field cooling over a more limited temperature range. Atomically disordered and weakly ordered alloys were used. The data indicate that the peak in susceptibility is due to the blocking of superparamagnetic clusters. Exchange anistropy effects can be attributed to the "spin-glass freezing" of antiparallel moments which results in the fixing of local anisotropy directions.

The paper is organized into five sections. Section II briefly describes the alloy preparation procedures and the magnetic measurement techniques. Section III presents experimental ac susceptibility and magnetization data and interpretation in terms of superparamagnetism and blocking. Section IV presents experimental data on the thermoremanent magnetization versus temperature upon warming from 4 K after various field-cooling conditions. These data are shown to be indicative of a strong freezing of local anisotropy directions near 35 K upon cooling in a field of 8 kOe. Data on the effects of weak atomic ordering and crystalline anisotropy on the spin freezing are included in this section. Section V presents an overall picture and considers various candidate models.

II. EXPERIMENT

Ni-Mn alloys of 24.6 at. % Mn were used in this study. The alloys were cast into ingots in an argon

atmosphere after rf induction melting. The ingots were then homogenized by cold working and quenching from 1000 °C several times. Spherical samples for measurement, 2.5–3.0 mm in diameter, were fabricated by the grinding procedure used by Carter *et al.*[8] and a two-pipe lapidary method, in which the sample was simultaneously ground and rotated about two orthogonal axes. Compositions were determined by atomic-absorption methods. To atomically disorder the spheres, they were vacuum encapsulated in quartz and homogenized at 1000 °C for at least 3 h. The quartz capsules were then plunged into ice water and simultaneously shattered with a brass mouse-trap device. The spheres were then electropolished. Weak atomic order was subsequently induced in some quenched samples by annealing in evacuated Pyrex capsules at 500 °C for a few minutes and quenching as above. Annealing times were taken to be cumulative.

Upon quenching, it is reasonable to expect the formation of some short-range chemical order.[9] Neutron diffraction on rod samples quenched from 1000 °C showed no long-range order but some short-range order, as evidenced by broad scattering at the superlattice angles. Annealing briefly at 500 °C is expected to increase the degree of short-range order (SRO) by increasing the size and number of SRO clusters.

In order to assess the role, if any, of crystalline anisotropy on the magnetic behavior, a single-crystal specimen of approximately 25 at. % Mn-Ni was obtained from a large-grained ingot. The ingot grains were revealed by an etch in warm ferric chloride (FeCl₃) solution. To substantially disorder the sample, it was homogenized at 1100 °C for 24 h; 1000 °C was not adequate due to the relative absence of voids, grain boundaries, and dislocations. Longer times would be required to achieve complete disorder. Neutron diffraction demonstrated that quenching from 1100 °C did not damage the single crystal.

Standard vibrating-sample magnetometry was used to measure thermoremanent magnetization (TRM), partial thermoremanent magnetization (PTRM), magnetization versus field, and magnetization versus temperature. Temperature was measured with a calibrated GaAs diode. Susceptibility measurements were made by a low-frequency, low-field ac induction method, as described in Refs. 10 and 11, using a carbon resistance thermometer calibrated to ± 10% accuracy.

III. SUPERPARAMAGNETISM AND BLOCKING

A. Low-field ac susceptibility

Figure 1 shows the internal ac susceptibility, measured at 20 Hz in a field of 2.5 Oe rms, as a function
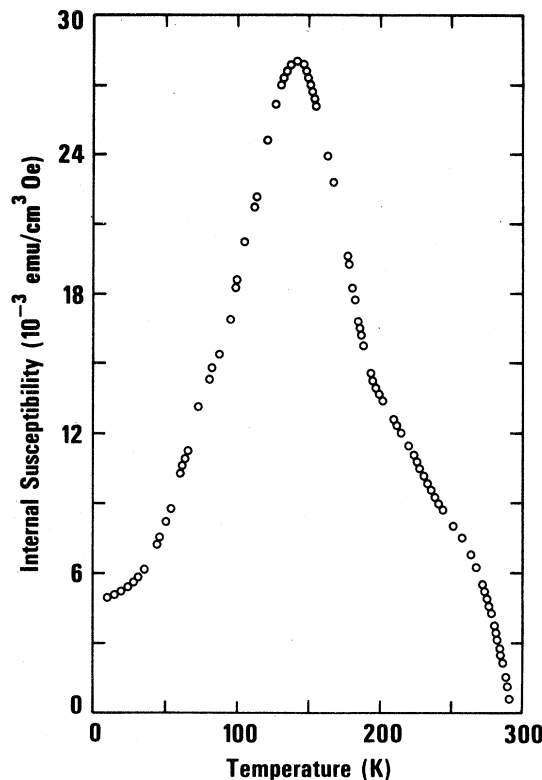

FIG. 1. Internal ac susceptibility at 20 Hz and 2.5 Oe rms vs temperature for a disordered 24.6 at. % Mn-Ni sample. Volume susceptibility, computed as emu/cm³ Oe, is dimensionless.

of temperature for a 24.6 at.% Mn-Ni sample. Three temperature regimes may be distinguished: above 260 K, 260 K down to the peak at 140 K, and below 140 K. A plot of the inverse susceptibility versus temperature, using the same data as in Fig. 1, is shown in Fig. 2.

The inflection point in susceptibility χ at 260 K in Fig. 1 and the corresponding rapid increase in $1/\chi$ above 260 K in Fig. 2 indicate that 260 K corresponds to the Curie point of the ferromagnetic components within the disordered alloy. Since the nominally disordered alloy contains regions of short-range order, and since ferromagnetism is a consequence of atomic order, it is reasonable to assign 260 K as the Curie point of these short-range ordered clusters based on the drop in susceptibility. This Curie temperature is quite different from the 725 K value for Ni₃Mn with complete long-range atomic order. The method of Arrott plots, often used to obtain the Curie temperature, tends to underestimate it near the 25 at. % Mn-Ni composition.[12]

The intermediate temperature regime from 260 K down to the peak temperature 140 K is most easily interpreted in terms of the variation in $1/\chi$ with tem-
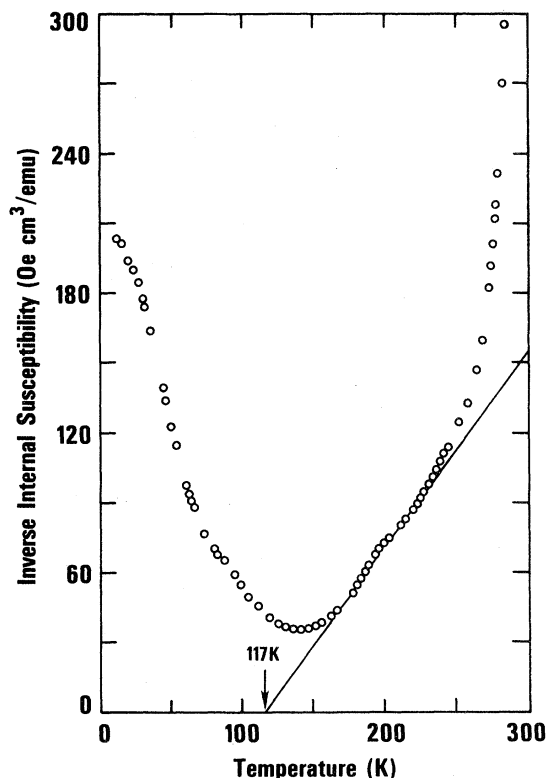
FIG. 2. Inverse internal susceptibility vs temperature for the same data as in Fig. 1.

perature for this region, shown in Fig. 2. The linear dependence is indicative of Curie-Weiss behavior, with a Weiss constant, or superparamagnetic Curie temperature θ, of 117 K and a Curie constant C of 1.18 K. The ratio θ/C yields a molecular field parameter γ of 99. These and additional results on superparamagnetism in this regime will be examined in Sec. III B.

The low-temperature regime below 140 K reveals a drop in the susceptibility. Given the indication of superparamagnetism above 140 K discussed above, one reasonable explanation for the falloff is the blocking of the superparamagnetic clusters along the lines proposed by Néel.[13-17] This and similar mechanisms have been proposed to explain the behavior of the susceptibility in mictomagnets and spin-glasses below the peak temperature.[7,18-22] Other mechanisms involving exchange coupling[23] and spin freezing[24,25] have also been proposed. These processes will be further examined in Secs. IV and V. Long-range antiferromagnetism as the source of the susceptibility peak is precluded in this and similar mictomagnetic—spin-glass alloys by neutron diffraction.[2]

B. Superparamagnetism with interactions

To further explore the superparamagnetic behavior over this intermediate temperature interval, the magnetization was measured versus field for various temperatures between 140 and 260 K. It is well known that in noninteracting superparamagnetic systems, the magnetization scales with the internal field—temperature ratio, H_{int}/T. For systems with interactions, as indicated by the nonzero temperature intercept in Fig. 2, the scaling might be expected to follow the effective field-temperature ratio H_{eff}/T, with

$$H_{eff} = H_{int} + \gamma M \quad , \tag{1}$$

where γ is the molecular-field parameter indicated in Sec. III A and M is the magnetization. The usual Langevin dependence of the magnetization may be expressed as

$$M = N\mu L\left(\mu H_{eff}/kT\right) \quad , \tag{2}$$

where $L(\alpha)$ is the Langevin function, μ is the moment per cluster, and N is the number of clusters per unit volume.

A plot of the magnetization M as a function of the parameter H_{eff}/T for a range of field values (0–8 kOe) and temperature values ($160 < T < 250$ K) is shown in Fig. 3 for $\gamma = 99$. The scaling of all the data over this range of temperatures makes a convincing case for superparamagnetic behavior with cluster interaction. The value of γ used to obtain these results was not obtained by a fitting procedure. Rather, it was obtained from the ac susceptibility data of Fig. 2, a completely different measurement. Values of γ which differ by as little as 10% give a noticeably poorer scaling.
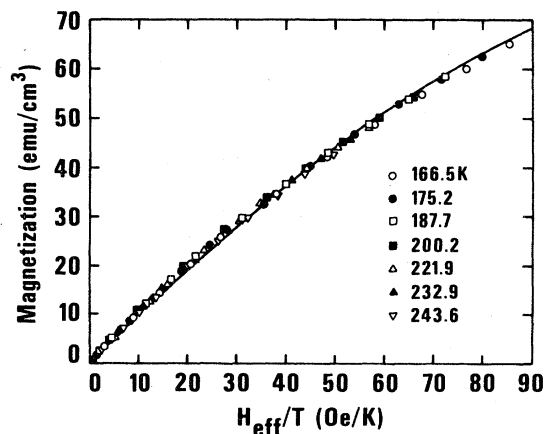

FIG. 3. Magnetization vs effective field H_{eff} and temperature T. The effective field was obtained from the molecular-field analysis discussed in the text. The curve is a Langevin equation with cluster moment and density derived from the data.

The data of Fig. 3 were further analyzed following the approach of van der Giessen,[26] modified to include cluster interactions, to obtain the cluster concentration N and average cluster moment μ. The method is based on the two operational equations

$$M = N \mu L (\alpha) \tag{3}$$

and

$$\alpha = \mu H_{\text{eff}} / kT \quad . \tag{4}$$

By taking logarithms, one obtains

$$\ln[L(\alpha)] = \ln(M) - \ln(N\mu) \tag{5}$$

and

$$\ln(\alpha) = \ln(H_{\text{eff}}/T) + \ln(\mu/k) \quad . \tag{6}$$

The analysis uses two plots: a master plot of $\ln[L(\alpha)]$ versus $\ln(\alpha)$ for $0.01 < \alpha < 22$ and a plot of $\ln(M)$ versus $\ln(H_{\text{eff}}/T)$ from the experimental data and value of γ. From Eqs. (5) and (6), the two plots superimpose if the data follow a Langevin function exactly. The shift in axes to achieve the superposition yields $\ln(N\mu)$ and $-\ln(\mu/k)$, thereby giving the cluster concentration N and cluster moment μ (compare Ref. 27).

Applied to the data of Fig. 3, the above procedure gives $N\mu = 123$ emu/cm³ (equal to the saturation magnetization) and $\mu = 349\mu_B$. These determinations were made graphically by giving equal weights to the high-field and low-field data. The Langevin equation [Eq. (2)] based on the above parameters is shown by the solid line in Fig. 3. As a result of the nonpreferential weighting, the data in Fig. 3 are above the curve for $H_{\text{eff}}/T < 45$ and below the curve for $H_{\text{eff}}/T > 45$. If preferential weighting were used, $N\mu$ could differ by up to 10% and μ by 20%. The available volume per cluster, $1/N$, is 2.6×10^{-20} cm³, corresponding to a (spherical) cluster separation of 37 Å, well within single-domain size. Assuming one μ_B per atom for ordered regions,[28] the cluster moment of $349\mu_B$ implies a spherical cluster size of about 20 Å. A better fit could be obtained by including a distribution in cluster sizes.[29] It is concluded that superparamagnetism with cluster interaction exists in the intermediate temperature regime.

C. Blocking of superparamagnetic clusters

In order to address the question of cluster blocking as a possible mechanism for the susceptibility falloff below 140 K, the frequency dependence of the peak position from 20 Hz to 20 kHz was examined. It is well known that a shift in the peak position to higher temperature as the frequency is increased provides evidence for a thermally activated process such as blocking. No change in the peak position could indi-

cate a genuine magnetic phase transition.

Susceptibility data in the vicinity of the temperature of the peak, designated by T_B, are shown in Fig. 4 for the disordered 24.6 at. % Mn-Ni specimen of Fig. 1. The data are normalized to one. The peak shifts to higher temperature as a function of frequency. For frequencies higher than 60 kHz, the skin depth of the sample is less than its radius, the imaginary component of the susceptibility is no longer approximately zero, and the ac losses become significant. The change in electrical resistivity with temperature $d\rho/dT$ near T_B is only 3×10^{-8} Ω cm/K.[30] Therefore the change in skin depth with temperature near T_B is negligible.

An increase in T_B with frequency may be taken as evidence for a thermally activated process such as blocking. However, the data in Fig. 4 show that the shift, while distinct, is quite small. A frequency increase by four orders of magnitude results in a peak shift of only 10 K. The small size of the shift indicates that the activation energy for the thermal process is rather large. This energy is easily estimated from the Néel blocking model, in which the relaxation time τ of a single-domain cluster is expressed as

$$\tau = \tau_0 \exp(E_a/kT) \quad , \tag{7}$$

where τ_0 is a constant and E_a is the thermal activation energy. A cluster blocks (i.e., its moment remains frozen in position) at that temperature (T_B) at which the measuring time t_{meas} equals the relaxation time. Thus,

$$\ln t_{\text{meas}} = \ln \tau_0 + (E_a/k)(1/T_B) \quad , \tag{8}$$

and a plot of $\ln t_{\text{meas}}$ versus $1/T_B$ yields a straight line. The measuring time t_{meas} is the reciprocal of the frequency of the susceptibility experiment. From Eq. (8) it is clear that a weak variation in T_B with t_{meas} corresponds to a large activation energy E_a.

An Arrhenius plot of $\ln t_{\text{meas}}$ versus $1/T_B$ for the data of Fig. 4 was found to be linear and yielded an
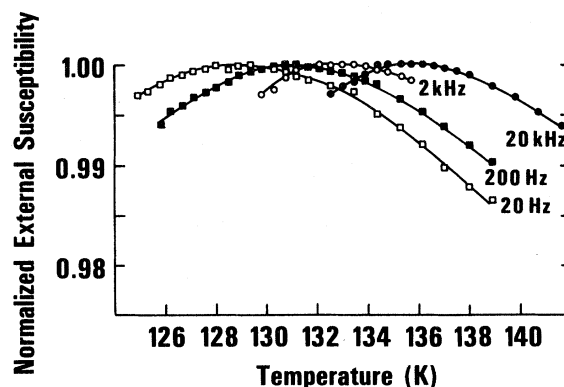

FIG. 4. Normalized ac susceptibility vs temperature of the sample of Fig. 1 as a function of frequency.

activation energy of 1.6 eV or 1.8×10^4 K.[10] While this is unphysically large, it is in line with activation energies estimated for a few other spin-glasses and mictomagnets. For example, energies of 6000—6400 K and 7500 K have been reported for 10 at. % Fe-Au,[31,32] and 4400 K for 0.94 at. % Mn-Cu.[33] No frequency dependence of T_B was found in 16.7 at. % Mn-Cu,[34,35] dilute Ag-Mn,[36] or slow-cooled Mn-Cu with less than 1.5 at. % Mn.[33]

The above results lend partial support to two hypotheses. On the one hand, the increase in T_B with frequency and the qualitative agreement with Eq. (8) support a Néel blocking model. On the other hand, the weak dependence of T_B on frequency and the corresponding large values of E_a can be interpreted as consistent with a genuine magnetic phase transition at T_B. Other results, however, support the former mechanism. The first of these concerns the effect of cluster size on the susceptibility peak magnitude, position, and width. The second is related to the observed onset of hysteresis below 140 K.

It is reasonable to attribute the broad character of the susceptibility peak to a distribution in cluster size and composition. The peak temperature T_B would correspond to the blocking of the larger clusters, with smaller clusters blocking at progressively lower temperatures. A distribution in cluster sizes and blocking temperatures is known to cause magnetic viscosity or after effect.[37] Such a "thermal fluctuation after effect" was investigated by Néel.[14,16] The distribution in cluster volumes and moments assures that, at any temperature near and below T_B, the relaxation time of *some* clusters is on the order of t_{meas}. Wohlfarth showed that the distribution in blocking temperatures could be calculated from the tempera-

ture dependence of the susceptibility, assuming a superparamagnetic blocking model.[38] Mulder *et al.* applied this method to Cu-Mn.[33] They found that, in the case of an alloy with a broad susceptibility peak, the maximum of the distribution occurred 20% below the susceptibility peak temperature. That is, most of the clusters blocked well below T_B.

In order to explore cluster size effects, a series of low-field susceptibility measurements were made for the 24.6 at. % Mn-Ni alloy as a funciton of atomic ordering by annealing the disordered alloy at 500 °C. It is well known that such ordering increases the size and concentration of short-range ordered clusters.[5] With increased atomic order, several effects were found[10]: (i) The peaks became broader; (ii) the peaks generally shifted to higher temperature; and (iii) the magnitude of the susceptibility at the peak χ_B increased. Various parameters derived from the susceptibility data for a single specimen with states of progressively greater atomic order are listed in Table I. As noted, both χ_B and T_B increase. The superparamagnetic Curie temperature θ and molecular field parameter γ are quite interesting in that they go from positive to zero to negative with order development. This indicates an increase in antiferromagnetic interactions, possibly between clusters, but probably between clusters and antiparallel spins in the matrix. For the "1-min" anneal, there is a balance between ferro- and antiferromagnetic interactions.

The above changes in the susceptibility peak with order development are supportive of the blocking hypothesis. The shift to higher temperature is due to the increased average cluster size (and moment). The increase in the peak width is due to the increase in the distribution of cluster sizes. The increase in

TABLE I. Maximum internal susceptibility χ_B, temperature of the susceptibility peak T_B, superparamagnetic Curie temperature θ, Curie constant C, and molecular-field constant γ for 24.6 at. % Mn-Ni, initially quenched (0 min) and annealed at 500 °C for the cumulated times shown. The values of θ, C, and γ were determined from plots of inverse internal susceptibility versus temperature as discussed in the text. The approximate superparamagnetic regimes are indicated. The data are all for a single specimen different from that of Fig. 1. (Annealing times only determine the degree of order relative to the quenched state. The maximum internal susceptibility χ_B is often a more reliable indicator of the degree of SRO.)

Annealing time at 500 °C (min)	χ_B	T_B (K)	θ (K)	C (K)	γ	Superparamagnetic regime (K)
0	0.016	109	105	1.77	59.5	160–250
1	0.019	129	0	2.86	0	160–260
3	0.081	170	−62	20.1	−3.08	180–240
7	0.108	164	−72	27.4	−2.63	180–250
11	0.122	161	−50	27.6	−1.81	180–255
15	0.134	163	−20	26.7	−0.75	185–260
30	0.177	164	−20	34.0	−0.59	175–250

χ_B is due to the increase in cluster moment. A shift in T_B with cluster growth was also reported by Volkenshtein et al.[39] Contrary to their measurements, however, the actual shape of the curves changes. After a few minutes of annealing, the susceptibility curves broaden as the alloy becomes more ferromagnetic. It is this broadening that prevents the actual peak from moving monotonically to higher temperatures.[10]

There is further evidence from hysteresis data that T_B corresponds to the initiation of blocking, associated magnetic viscosity, and relaxation effects. After cooling an initially demagnetized sample to 4 K in zero field, hysteresis loops were measured at discrete temperatures as the sample was warmed to 300 K. The maximum field amplitude was 8 kOe. The hysteresis loss for each M-H loop was calculated and the values are plotted in Fig. 5. It is notable that hysteresis loss is almost zero above T_B. Below T_B, the hysteresis increased gradually. During the measurement of magnetization, relaxation effects were quite obvious below 140 K. Presumably, if sufficient time were allowed after changing the field, the hysteresis would disappear. For these measurements, 20–30 sec were allowed per datum. Each quarter of a hysteresis loop involved 21 data points.
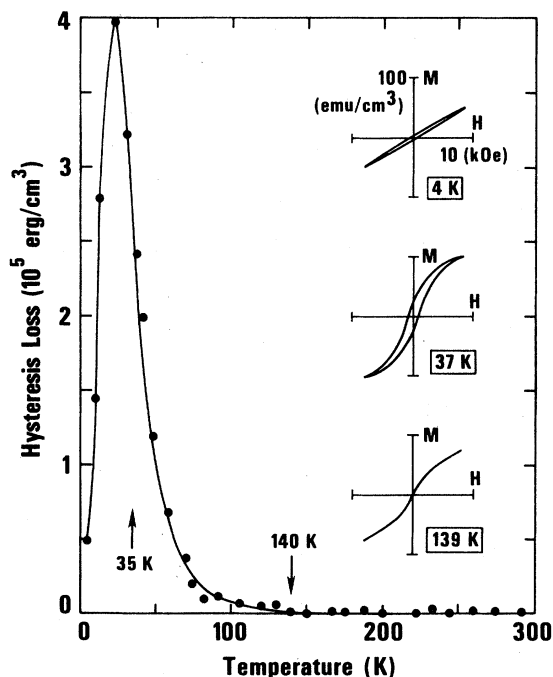
The hysteresis reaches a maximum near 35 K, the temperature to be labeled T_A. It is expected that T_A would be a function of the characteristic field, in this case 8 kOe. Below this temperature, the character of the magnetization curves changes, as illustrated in the insets. The values of the magnetization are lower and hysteresis is proportionately less. It would appear that a second transition appears near T_A, to be discussed in Sec. IV.

This same trend in the hysteresis was noted by Kouvel in Cu-Mn, Ag-Mn, and other mictomagnetic alloys.[40] Viscosity and magnetic aftereffects have been previously measured in well-annealed Ni-Mn alloys quenched from 500 °C and lower temperatures.[41] These effects were noted between 300 and 400 K and were attributed to relaxation of the magnetization of the long-range ordered phase.

Large thermal activation energies are not necessarily proof of a magnetic phase transition. They could be accounted for by the exchange coupling between clusters based on their close proximity as calculated in Sec. III B, or between clusters and matrix spins, and related to the "extraordinary" viscosity associated with exchange anisotropy by Jacobs and Kouvel.[42] This stronger process and the related problem of low-temperature moment freezing are the subject of Sec. IV.

FIG. 5. Hysteresis loss for an external field cycled between ±8000 Oe vs temperature upon warming after cooling the sample of Fig. 1, initially demagnetized, to 4 K in zero field. The insets show the shapes of typical M-H loops at three temperatures.

IV. EXCHANGE ANISOTROPY AND FREEZING

A. Thermoremanent magnetization

The peak in the hysteresis loss at 35 K in Fig. 5, for the disordered 24.6 at% Mn-Ni alloy cooled to 4 K in zero field, indicates the occurrence of a strong freezing process at low temperature. As is well known, when disordered Ni-Mn is cooled in an external magnetic field to liquid-helium temperatures, a unidirectional anisotropy is induced in the field direction, characterized by a shifted hysteresis loop and a thermoremanent magnetization (TRM).[2,43] If the alloy is then warmed in zero field, the TRM simply decays to zero, as expected. An exception is the case of weakly ordered Ni₃Mn which exhibits TRM reversal upon warming.[6,44] The shifted hysteresis loop, reversible at liquid-helium temperatures, gradually shifts back to the origin upon warming to about 35 K.[2] This section discusses the thermoremanent magnetization as a funciton of field history and temperature, as well as other pertinent magnetization data which serve to elucidate the nature of the low-temperature freezing process.

TRM and partial thermoremanent magnetization (PTRM) data for the sample of Fig. 1 are shown in Fig. 6. The specimen was initially demagnetized before each set of measurements. In measuring PTRM, the cooling field, in this case 8000 Oe, was
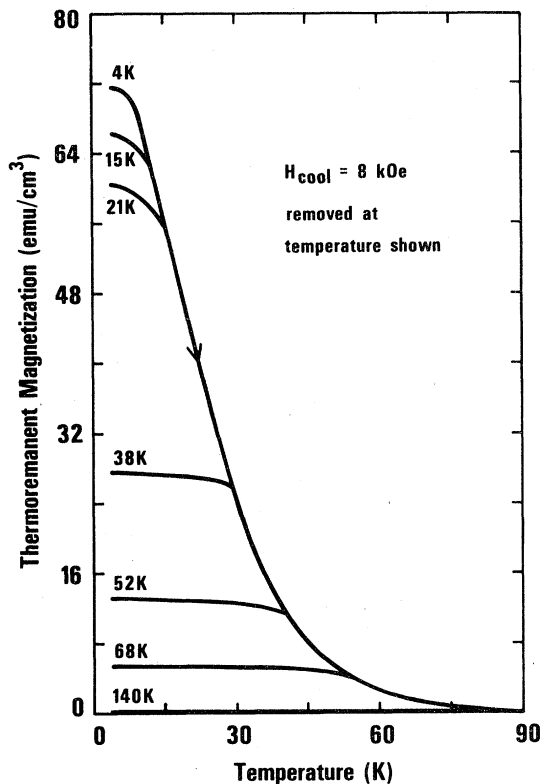
FIG. 6. Thermoremanent magnetization (TRM) and partial thermoremanent magnetization (PTRM) upon warming from 4 K after cooling in 8000 Oe from room temperature to the temperatures indicated. The sample is the disordered Ni_3Mn specimen of Fig. 1.

applied over a limited temperature range between 300 and 4 K. The uppermost curve, labeled "4 K," shows the ordinary TRM warming curve. The other warming curves represent PTRM, for which the cooling field was removed at the temperatures shown, and the samples further cooled to 4 K in zero field. All TRM and PTRM measurements were made upon warming from 4 K after the indicated field cooling procedure was complete. For the actual measurements, the electromagnet was removed from the vicinity of the magnetometer to avoid any residual fields.

There are three important features in Fig. 6. First, the warming PTRM curves all intersect the TRM curve for 4 K and follow it to zero at high temperature. Second, if the cooling field is removed at any temperature above 140 K (i.e., T_B), the PTRM is zero. These results are very suggestive of blocking, beginning gradually at T_B and increasing in effect at lower temperatures. Third, it is seen that the PRTM at 4 K increases abruptly as the field cut-off temperature is reduced from 38 to 21 K. This jump is an indication of the stronger freezing process which sets in

at low temperature. The PTRM at 4 K are replotted in Fig. 7 as a function of the temperature at which the cooling field was switched off, as indicated by the open circles and curve labeled $PTRM_1$. The rapid increase at about 35 K is clearly evident.

A second set of PTRM measurements was carried out in which a cooling field of 8 kOe was turned on during cooling at the indicated temperature and kept on down to 4 K. The field was then switched off and the thermoremanence measured. These data are indicated in Fig. 7 by the solid circles and the curve labeled $PTRM_2$.

The first set of PTRM measurements is suitable for the demonstration of blocking, however the second set is not. While TRM due to blocking has been known in rock magnetism for some time, it is a weak remanence which can be overcome by external fields greater than the cluster or particle coercive force. A field of 8000 Oe applied below an individual cluster's blocking temperature should be much larger than the cluster's coercive force, usually no more than approximately 1000 Oe,[45] and more than enough to orient the cluster moment in the field direction. If blocking were the only process occurring, the $PTRM_2$ curve (filled circles) should be flat, or at best have a small positive slope. This is the case down to 50 K. However, there is a knee at about 35 K. This indicates that a freezing process much stronger than
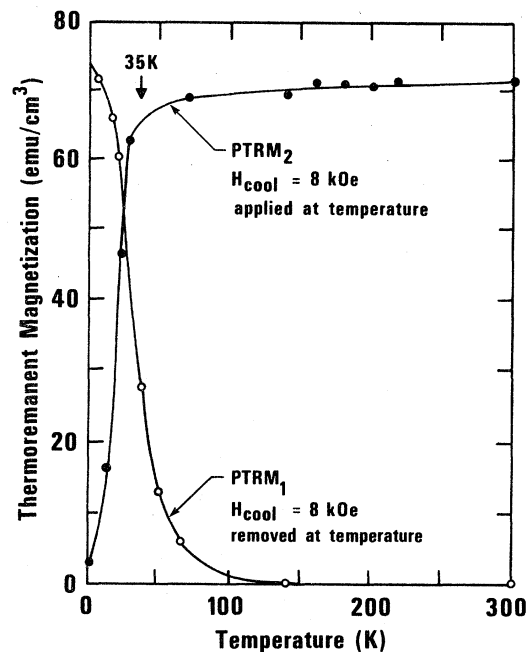

FIG. 7. Partial thermoremanent magnetization (PTRM) at 4 K after an 8000 Oe cooling field was removed ($PTRM_1$) or applied ($PTRM_2$) at the temperature indicated on the abscissa. The $PTRM_1$ data are from Fig. 6.

blocking takes place below 35 K with respect to the 8 kOe experimental field. This same freezing process must also be reflected in the first set of PTRM data (open circles). Therefore, a large portion of the effects seen in Fig. 6 is not due to blocking alone. This is seen in the large gap between the warming curves for 21 K (< 35 K) and 38 K (> 35 K), noted above. The 35 K temperature will be labeled T_A. This is the same temperature at which the hysteresis loss was found to show a peak (Fig. 5).

The effect of temperature on the TRM has been discussed. At this point, the effect of cooling field on the TRM will be examined. Figure 8 shows the TRM obtained by field cooling to 4 K as a function of cooling field for a single 24.6 at. % Mn-Ni sample in the atomically disordered state, and for weak order after annealing at 500 °C for the times indicated. The specimen is the same as the one featured in Table I. The data of the disordered sample, labeled "0 min," show a simple monotonic increase in the TRM with cooling field. This is in agreement with previous results.[2] With weak ordering, however, the shape of the TRM—cooling field curves changes radically.[6] Figure 8 shows that the TRM increases to a maximum for cooling fields of about 600 Oe and then decreases. *The negative slopes in the TRM curves of Fig. 8 correlate with the negative molecular-field coefficients of Table I.* In addition, the TRM for the larger cooling fields initially decreases as ordering is initiated and then increases for annealing times in excess of about 3 min. For well-ordered alloys, the TRM is known to be smaller.[6]
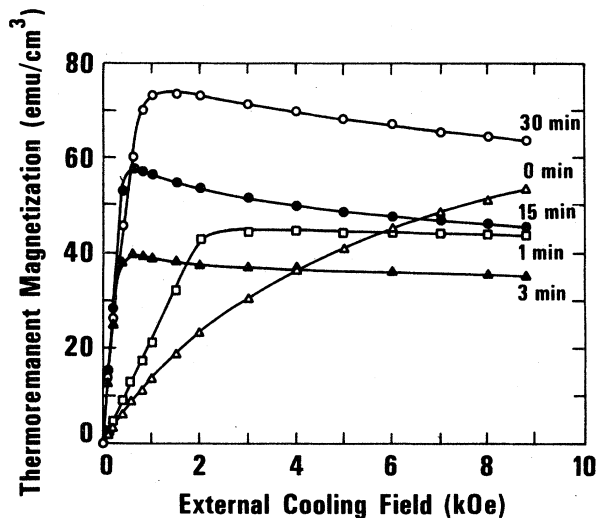
Similar maxima and negative slopes in TRM versus cooling fields have been seen in other micto-magnetic—spin-glass compounds. These are $Au_{0.995}Fe_{0.005}$ (Ref. 18), $Pt_{0.99}Mn_{0.01}$ (Ref. 46), disordered $Cu_{0.91}Mn_{0.09}$ (Ref. 47), $Cu_{0.92}Mn_{0.08}$ (Ref. 48), $(Eu_{0.3}Sr_{0.7})S$ (Ref. 49), $(La_{0.98}Gd_{0.02})Al_2$ (Ref. 50), and $Au_{0.958}Fe_{0.042}$ (Ref. 51).

B. Frozen-in superparamagnetic state

It is evident from the above data that a strong freezing process occurs at about 35 K. From the negative effect of cooling field on the TRM in Fig. 8, it is also evident that large cooling fields align antiparallel moments in partially ordered specimens.

Additional measurements have been made which further elucidate the above freezing process. The results are shown in Fig. 9, where two very different kinds of data are compared. The solid lines correspond to the data of TRM at 4 K versus cooling field, Fig. 8, with the curve for 30 min annealing excluded for the sake of clarity. The cooling fields on the
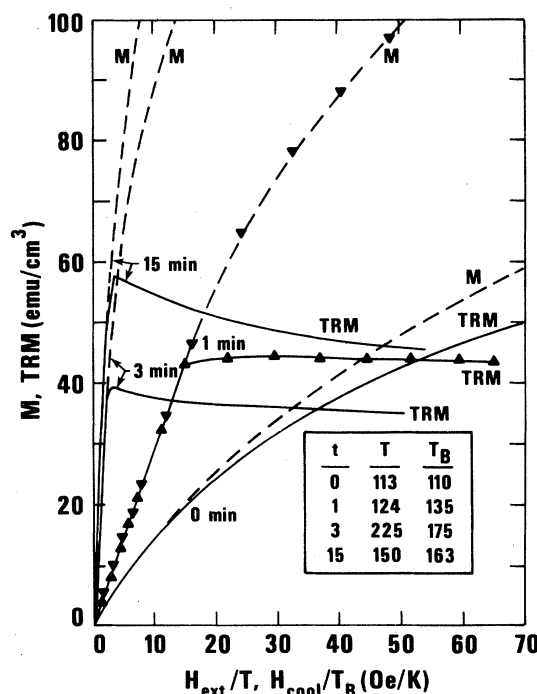

FIG. 9. Thermoremanent magnetization TRM vs cooling field H_{cool} scaled by the blocking temperature T_B (solid curves); and magnetization M vs measuring field H_{ext} scaled by the temperature T at which the data were taken (broken curves). The cumulated annealing times at 500 °C after the disordered state are shown for each pair of curves. Except in one instance, data points are omitted for the sake of clarity.

FIG. 8. Thermoremanent magnetization at 4 K as a function of cooling field for a 24.6 at % Mn-Ni sample. The cumulated annealing times at 500 °C for the initially disordered alloy are indicated. (After Ref. 10.)

abscissa have been scaled by the blocking tempera-
tures appropriate in each instance, as indicated by the
T_B values in the inset. The broken curves, however,
represent data of magnetization M versus external
field H_{ext} measured at temperatures close to T_B, as
indicated by the T values listed in the inset. Thus,
this figure compares the TRM at 4 K for a range of
cooling fields with the magnetization at approximately
T_B, just at the onset of blocking, as a function of the
applied external field.

The results are quite remarkable. For each set of
data for a given specimen, the two curves superim-
pose at low field. That is, for fields below some criti-
cal value the effect of cooling field on the TRM at 4
K is the same as the effect of the external field on
the induced magnetization at the blocking tempera-
ture.

Néel's theory for blocking of single-domain parti-
cles suggests that the TRM results from the blocking
of superparamagnetic grains or clusters.[13] According
to Néel's theory,[17,52] the TRM (M_{TR})at some tem-
perature T (e.g., 4 K) after cooling to that tempera-
ture in a field H_{ext} is given by

$$M_{TR}(T,H_{ext})$$
$$= M_s(T) \int_0^{\pi/2} \tanh(a\cos\theta)\sin\theta\cos\theta \, d\theta \quad , \quad (9)$$

where a is defined as $\mu(T_B)H_{ext}/kT_B$ and M_s is the
saturation magnetization of the aligned super-
paramagnetic clusters at temperature T. The cluster
moment at the blocking temperature is $\mu(T_B)$. The
integral cannot be evaluated in closed form. For
small values of a, the tanh function can be expanded
in a power series. In this limit the integral yields

$$M_{TR}(T,H_{ext}) = M_s(T)(\tfrac{1}{3}a - \tfrac{1}{15}a^3 + \tfrac{2}{105}a^5 - \cdots) \quad .$$
$$(10)$$

The magnetization as a function of temperature
and field for Langevin superparamagnetism is given
by

$$M(T) = M_s(T)(\coth\alpha - 1/\alpha)$$
$$= M_s(T)(\tfrac{1}{3}\alpha - \tfrac{1}{45}\alpha^3 + \tfrac{2}{945}\alpha^5 - \cdots) \quad , (11)$$

where α is defined as $\mu(T)H_{int}/kT$. The functional
similarity of the terms in Eqs. (10) and (11) is ap-
parent. The functions for TRM [Eq. (9)] and super-
paramagnetism [Eq. (11)] are roughly coincident for
small a and α, but gradually diverge for $a \approx \alpha \gtrsim 1$.
The curves in Fig. 9 confirm that cooling below the
blocking temperature freezes-in the superparamagnet-
ic state for cooling fields below about 600 Oe (depen-
dent upon annealing state). For larger cooling fields
this is not the case. The curves in Fig. 9 bifurcate
when the antiparallel moments in the alloy become
aligned opposite to the cooling field. This effect, of
course, was not predicted by Néel's TRM theory or
ordinary superparamagnetism.

C. Low-temperature freezing

In Fig. 10, the magnetization upon warming from 4
K, after cooling from room temperature to 4 K in
zero field, are shown for different values of the
external dc field H_{ext} from 10 Oe to 8 kOe. The
magnetization values were divided by the internal
field H_{int} to facilitate comparison of the four curves.

It is evident from Fig. 10 that larger and larger
measuring fields are required to shift the peak to
lower and lower temperatures. Earlier work indicates
that the peak does not shift below about 35 K even
for fields of 15 and 30 kOe, though the peak is
suppressed for 50 kOe.[4] The magnetization peak
temperature for different measuring fields $T_B(H)$ in
Fig. 10 do not follow the Néel relation for blocking[53]

$$[T_B(H)/T_B]^{1/2} = (1 - H/H_K) \quad , \quad (12)$$

where T_B is the blocking temperature in the limit of
zero field and H_K is the anisotropy field which may
be taken to be approximately 50 kOe. It is also clear,
from the perspective of superparamagnetism, that a
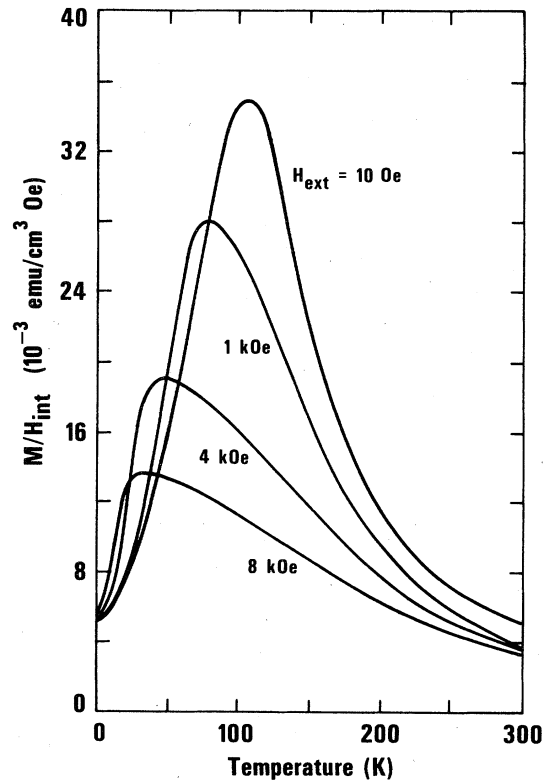much stronger process than blocking is involved

FIG. 10. Magnetization upon warming after zero-field
cooling for different dc measuring fields. The magnetization
values have been scaled by the internal fields at each
measuring temperature. The sample is the same as in
Fig. 1.

here. Blocking is with respect to temperature and field. The thermal equivalent of 8 kOe, using the simple product μH and the average cluster moment of 349 μ_B from Sec. III B, is 188 K, which should be sufficient to unblock clusters even at 4 K.

The set of curves in Fig. 10 differ from those of Kouvel *et al.*[54] This is simply because in that work, and in subsequent publications, the values of M at different internal fields were determined by interpolation from a single hysteresis loop at each temperature obtained by cycling the field between ± 8 kOe. In those studies, then, the characteristic external field was 8 kOe, and all curves peaked at the same temperature.

The nature of the 35 K freezing can be further illuminated by examining a weakly ordered alloy. Annealing a disordered Ni_3Mn alloy for a few minutes at 500 °C is expected to increase the degree of SRO by increasing the size and number of SRO clusters. This is referred to as "weak order." The effects of this brief annealing are rather unusual. It was found that the TRM, measured upon warming from 4 K in zero field after field cooling, undergoes a reversal in direction.[6,44] Figure 11 presents the results for two kinds of remanence measurements on another 24.6 at.% Mn-Ni specimen, annealed for 11 min at 500 °C. The $PTRM_2$ data (solid circles) have the same meaning as in Fig. 7. The sample was cooled from 300 to 4 K, the cooling field of 8 kOe was switched off, and the remanence, $PTRM_2$, was measured. The other set of points (open circles) corresponds to the value of the maximum reversed remanence, MRRM, obtained upon warming from 4 K, following the $PTRM_2$ determination. For both sets of data the temperature

on the abscissa refers to the temperature at which the 8 kOe field was switched on during the initial cool down. Thus, each pair of points represents one complete field-cooling experiment.

Figure 11 shows unusual results when the cooling field was switched on below 35 K. The $PTRM_2$ is seen to rise to a sharp peak while the MRRM does not appear at all. These results may be explained in terms of cluster blocking and antiparallel moment freezing. The MRRM in weakly ordered alloys may be taken as a partial measurement of the viscous spins aligned antiparallel to the cooling field. It is quite small. It is apparent from the MRRM curve of Fig. 11 that 35 K corresponds to the freezing of these antiparallel moments with respect to the 8 kOe field. For cooling fields switched on below 35 K, they are already frozen in randomly and cause no MRRM. As these moments freeze randomly, moreover, superparamagnetic clusters can contribute more effectively to the positive TRM at 4 K so the $PTRM_2$ increases as the MRRM goes to zero. As the field switch-on temperature is made lower, the clusters themselves tend to freeze, thereby reducing the $PTRM_2$.

The role of anitparallel moments in weakly ordered Ni-Mn is also apparent from Figs. 8 and 9, as briefly mentioned in Sec. IV B. These figures show that under noninterrupted field cooling conditions (i.e., normal TRM data), large cooling fields are more effective in aligning the antiparallel moments prior to their freezing. The result in Figs. 8 and 9 is a decrease in TRM for cooling fields above 600 Oe or so. The large magnitude of this decrease also indicates that some clusters might be *ferromagnetically* coupled to individual antiparallel spins.

T_A refers to the temperature at which the antiparallel spins freeze with respect to the characteristic field. Owing to the viscosity of these spins, they appear to be always frozen with respect to fields up to about 600 Oe, depending on annealing state, as seen in Fig. 8. Therefore, it cannot be said that T_A equals $T_B(H)$ for fields less than 600 Oe, or that T_A corresponds to T_B in the limit of very small fields.

D. Role of crystalline anisotropy

There has been speculation about the role of crystalline anisotropy in mictomagnetic ordering.[1] A crystalline easy axis, for example, could stabilize the antiparallel moments in evidence above or provide the anisotropy for the blocking of clusters. The extent of such interactions may be examined by field-cooling experiments on single crystals.

Such experiments were carried out on a substantially disordered single crystal Ni_3Mn sphere. Shifted hysteresis loops measured at 4 K after field cooling in 8000 Oe were identical, regardless of whether the cooling (and measuring) field axis was [100], [111],
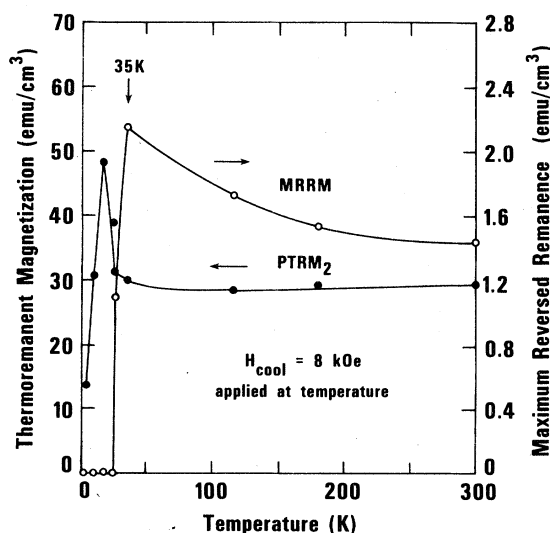

FIG. 11. Partial thermoremanent magnetization ($PTRM_2$) at 4 K, and maximum reversed thermoremanent magnetization (MRRM) upon warming for a weakly ordered alloy.

or [110]. This confirms the results of Yermolenko
and Turchinskaya who observed that the unidirec-
tional anisotropy constant was independent of field-
cooling direction.[55] In another set of measurements,
TRM was measured as a function of warming after
prior field cooling in 8000 Oe. The results are shown
in Fig. 12. The data exhibit a small bump at 90 K
and a small amount of remanence reversal above 160
K, but there was no dependence on field-cooling
direction.

Additionally, crystalline anisotropy does not affect
the blocking of clusters. An amorphous ribbon of
composition $(Ni_{0.8}Mn_{0.2})_{75}P_{16}B_6Al_3$ was measured at
low temperature.[56] The magnetization in a dc field
of 500 Oe after zero-field cooling had a broad peak at
28 K, reminiscent of disordered Ni_3Mn. The falloff
below 28 K was suppressed by field cooling in 500
Oe. Similar results were shown by Obi et al.[57]

The above conclusions are in accord with other
results on Ni-Mn. From the work of Blanchard and
Tutovan,[58] Satoh et al.,[59,60] and Murakami,[61] the
crystalline anisotropy is disordered Ni-Mn near the 25
at.% Mn composition is very small, and the tempera-
ture dependence down to at least 77 K is also small.
It is not expected to crystalline anisotropy changes
would be a cause of the features seen in the suscepti-
bility versus temperature curves. These experiments
refute the theory that crystalline anisotropy plays a
role in establishing the easy direction upon field cool-
ing. Hysteresis and torque measurements on single-
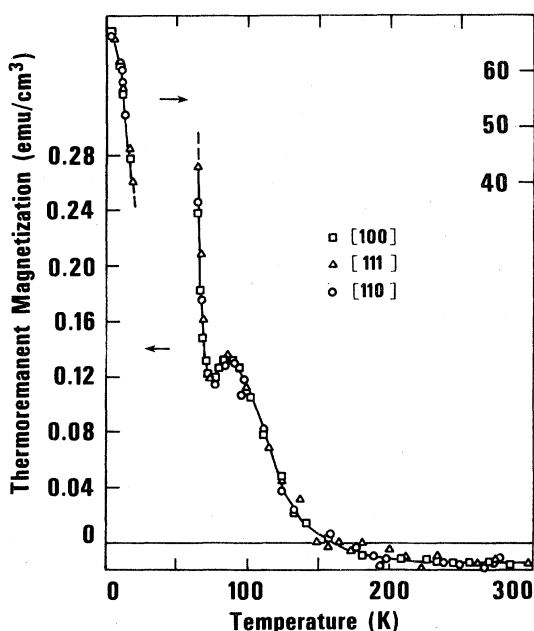crystal Cu-Mn gave the same conclusion.[62]

FIG. 12. Thermoremanent magnetization for single-
crystal Ni_3Mn upon warming after field cooling to 4 K in
8000 Oe along the three major crystal axes.

V. DISCUSSION

A. Superparamagnetism and spin-glass freezing

The previous two sections presented data on sus-
ceptibility and magnetization which indicate the oc-
currence of two processes: blocking of super-
paramagnetic clusters and freezing of certain an-
tiparallel moments. The antiparallel moments are be-
lieved to consist of Mn spins, which provide the local
anisotropy, and possibly small clusters ferromagneti-
cally coupled to them in weakly ordered alloys.

Quenching Ni_3Mn from 1000 °C after homogeniza-
tion results in a nominally disordered state which
inevitably contains short-range ordered (SRO) clus-
ters due to composition fluctuations and atomic dif-
fusion during the quench. Weak atomic order occurs
when such disordered alloys have been annealed at
500 °C for a few minutes. The SRO clusters are
small, single-domain and ferromagnetic, have a Curie
temperature near 260 K, and behave superparamag-
netically, with some interaction, between 160 and
250 K.

For temperatures below about 140 K, the clusters
begin to block, following a Néel model, in local an-
isotropy fields determined by viscous companion an-
tiparallel Mn spins to which they are exchange cou-
pled. Since ferromagnetism in Ni_3Mn is a conse-
quency of atomic order, the SRO clusters are expect-
ed to contain few if any antiparallel Mn moments.
The blocking of the clusters causes the susceptibility
to decrease and hysteresis to appear below 140 K.
The large activation energy associated with the sus-
ceptibility peak is indicative of large anisotropy fields.
Exchange anisotropy between the superparamagnetic
clusters, or between the clusters and the viscous an-
tiparallel Mn spins, would account for such anisotropy
fields.

As the temperature is further reduced, the viscous
antiparallel Mn moments themselves freeze at about
35 K. *Freezing is always with respect to field as well as
temperature;* 35 K appears to be a limiting value for
moderate fields.[63] The spin freezing also causes a
freezing of the local anisotropy for the superparamag-
netic clusters.

The existence of antiparallel moments and their
viscosity are amply demonstrated by thermoremanent
magnetization reversal[6] and the fact that a threshold
field is required for their antiparallel alignment (Fig.
8). The decrease in the TRM for cooling fields
greater than about 600 Oe suggests that annealing at
500 °C produces, in addition to the nucleation and
growth of "soft" superparamagnetic clusters, a popu-
lation of "hard" moments antiparallel to the net
magnetization which tend to reduce the TRM. The
soft clusters align in fields smaller than ∼600 Oe,
while the hard moments require fields greater than
∼600 Oe. It is not surprising that thermoremanent

magnetization reversal does not occur for cooling fields less than about 600 Oe.[6] That the antiparallel moments are Mn is supported by the NMR work of Kitaoka et al.[64] Because the freezing of the antiparallel moments is believed to involve single spins rather than clusters, it is termed a "spin-glass" freezing; the term "blocking" is not suitable because blocking involves clusters freezing in an anisotropic direction. It is questionable whether single moments can "block" in this classical sense.[65] The source of the spin viscosity is beyond the scope of this work, but is possibly an integral feature of spin-glasses.

The processes which occur during field cooling, which give rise to thermoremanent magnetization and shifted hysteresis loops, are as follows. During field cooling, the superparamagnetic clusters are aligned by the field once temperature drops below 260 K, the Curie temperature for the SRO clusters. If the cooling field is greater than about 600 Oe, the superparamagnetic clusters are aligned well enough to expose the viscous antiparallel Mn to a large negative effective field due to exchange coupling. This aligns the antiparallel moments opposite to the cooling field direction. Thus, clusters could be a requirement for antiparallel alignment of the Mn spins. They do seem to be necessary for susceptibility cusps and unidirectional anisotropy.[56,66,67] As temperature falls below 140 K, the superparamagnetic clusters begin to block in an anisotropic direction determined by the viscous antiparallel Mn. This is a weak freezing process. Near 35 K, the antiparallel moments freeze opposite to the direction of the cooling field. This is a strong freezing process and may be termed a "spin-glass" freezing as discussed above. Since the net moment of the antiparallel Mn spins is small,[6] displaced hysteresis loops, obtained after field cooling, are symmetrical in magnetization within experimental accuracy.

B. Other models

Some recent interpretations of mictomagnetic — spin-glass effects in alloys deserve comment. The first is that of Beck.[1,24] In his model for mictomagnetic alloys, the peak in low-field susceptibility corresponds to the freezing temperature of small (i.e., not cluster) moments located within a matrix. Clusters are exchange coupled to the spins of this matrix below the peak temperature and behave superparamagnetically above.[34] Due to exchange interaction, the clusters become gradually immobilized with decreasing temperature. The peak in susceptibility corresponds to the appearance of exchange anisotropy upon cooling, as suggested by Kouvel.[3]

The present model for Ni-Mn is similar to Beck's. However, one would have to postulate antiparallel moments for the spin matrix to account for TRM re-

versal and the maximum in TRM versus cooling field. In the present work, T_A is the freezing point of the antiparallel spins with respect to the characteristic experimental field. That is, during field cooling, the alloy must be cooled through T_A (rather than T_B) to obtain a stable shifted hysteresis loop between positive and negative fields equal to the cooling field.[10] The present model does not require T_B to be the spin-freezing temperature, but only the temperature at which blocking first appears upon cooling.[63]

Along the same lines as Beck's is the general mechanism proposed by Knitter et al.[47] which recalls the early work of Kouvel.[3] This involves antiferromagnetic-like regions with no net moment clamped to the lattice possibly by a local anisotropy. The source of this local anisotropy is not yet determined. Ferromagnetic regions are exchange-coupled to the antiferromagnetic-like regions, the latter providing the effective field necessary for displaced hysteresis loops. Knitter et al. discount the possibility of local anisotropy as a cause for the displaced loop due to the loop's symmetry in magnetization. However, as noted in Sec. IV C, the magnitude of the total antiparallel Mn spin moment, which is believed to provide the local anisotropy, can be very small. Also, TRM reversal and the maximum in TRM versus cooling field is accounted for by such local anisotropy.

The local environment model used by Satoh et al.[4,6] for exchange anisotropy and TRM reversal was based on the existence of antiparallel Mn atoms, but superparamagnetism was not considered. An extension of that model can explain the additional experimental results of the present study. The superparamagnetic clusters are assumed to be ferromagnetically coupled to the nearest-neighbor environment of the antiparallel Mn atoms, and the antiparallel Mn moments are assumed to be highly viscous.

Another interpretation is a blocking model adapted by Löhneysen and Tholence to explain the maximum and negative slope in TRM versus cooling field in $(La,Gd)Al_2$.[50] According to this blocking model, larger clusters block at higher temperatures than smaller clusters. While the larger clusters block in the direction of the external field, the smaller clusters block in the direction of the local effective field, which includes the negative dipolar-like fields of the already blocked clusters. This could result in a negative contribution to the TRM. Consequently the TRM versus cooling-field curve has a negative slope.

There are only two difficulties with respect to Ni₃Mn. One is that, upon warming, the negatively blocked clusters would unblock before the positively blocked larger clusters. For remanence reversal to occur, one would additionally have to hypothesize a large viscosity for the smaller clusters. The second difficulty is that large cooling fields should be much greater than any local fields unless they are exchange

fields, and the TRM should eventually increase for moderately high cooling fields. In fact, the TRM merely levels off and does not increase for cooling fields as large as 56 kOe.[6] This shows that effects much stronger than classical blocking occur in Ni_3Mn.

The small frequency dependence of the susceptibility peak temperature in certain mictomagnets has been discussed by other authors. Beck attributes the lack of a frequency dependence to a well-defined freezing of short-range antiferromagnetic spin order in a matrix.[68] Viscous magnetic behavior results from the interaction of magnetic clusters with the frozen matrix spins. Hardiman has observed that a weak frequency dependence is seen in those alloys in which the nearest-neighbor impurity coupling is antiferromagnetic.[69] Gray has suggested that a frequency dependence is seen only if the applied ac field is above a certain threshold value.[35] Other recent discussions are those of Murani[70] and Tholence.[71] Zibold and Korn have suggested that a frequency dependence is seen when clustering is present.[66] Finally, Cywinski and Gray conclude that the peak temperature becomes less frequency dependent as a distribution in activation energies broadens.[72]

VI. CONCLUSION

Measurements of susceptibility versus temperature, magnetization versus temperature, hysteresis, and thermoremanent magnetization have been made on disordered and weakly ordered Ni_3Mn alloys. The low-field, low-frequency ac susceptibility and moderate-field dc magnetization of disordered Ni_3Mn demonstrate superparamagnetism with cluster interaction below room temperature. The susceptibility peak at 140 K corresponds to the onset of relaxation

effects in these clusters upon cooling. The clusters originate from inherent short-range atomic order. The molecular-field constant, determined from the susceptibility data, goes from positive to zero to negative as a function of atomic ordering, indicating an increase in antiferromagnetic interactions. Thermoremanent magnetization (TRM) measurements as a function of cooling field show that, in weakly ordered alloys, there is a population of "hard" antiparallel moments which align opposite to the cooling field. The appearance of these antiparallel moments, the cause of decreasing TRM with increasing cooling field, correlate with the negative molecular-field constants for weakly ordered alloys. TRM measurements on a weakly ordered Ni_3Mn specimen show that 35 K is the freezing temperature of the antiparallel moments in the alloy with respect to an experimental field of 8 kOe. The large viscosity of these antiparallel moments, and the coupling of the superparamagnetic clusters to them, are believed to be the source of the remarkable mictomagnetic—spin-glass effects noted in this alloy system.

ACKNOWLEDGMENTS

*Present address: National Bureau of Standards, Boulder, Colo. 80303.

[1]P. A. Beck, Prog. Mater. Sci. 23, 1 (1978).

[2]J. S. Kouvel and C. D. Graham, J. Phys. Chem. Solids 11, 220 (1959).

[3]J. S. Kouvel, J. Phys. Chem. Solids 24, 795 (1963).

[4]T. Satoh, R. B. Goldfarb, and C. E. Patton, J. Appl. Phys. 49, 3439 (1978).

[5]M. J. Marcinkowski and N. Brown, J. Appl. Phys. 32, 375 (1961).

[6]T. Satoh, R. B. Goldfarb, and C. E. Patton, Phys. Rev. B 18, 3684 (1978).

[7]E. P. Wohlfarth, Physica 86—88B, 852 (1977).

[8]J. L. Carter, E. V. Edwards, I. Reingold, and D. L. Fresh, Rev. Sci. Instrum. 30, 946 (1959); J. N. Paranto and C. E. Patton, Rev. Sci. Instrum. 52, 262 (1981).

[9]S. Crane and H. Claus, Solid State Commun. 35, 461 (1980).

[10]R. B. Goldfarb and C. E. Patton, J. Appl. Phys. 50, 7358 (1979).

[11]R. B. Goldfarb, Ph.D. thesis (Colorado State University, 1979) (unpublished).

[12]H. Tange, T. Tokunaga, and M. Goto, J. Phys. Soc. Jpn. 45, 105 (1978). Compare: J. S. Kouvel, J. Phys. Chem. Solids 16, 127 (1960).

[13]L. Néel, Adv. Phys. 4, 191 (1955).

[14]L. Néel, C. R. Acad. Sci. 228, 664 (1949).

[15]L. Néel, Ann. Geophys. 7, 90 (1951).

[16]L. Néel, Rev. Mod. Phys. 25, 293 (1953).

[17]L. Néel, in Low-Temperature Physics, edited by C. DeWitt, B. Dreyfus, and P. G. deGennes (Gordon and Breach, New York, 1962), p. 411.

[18]J. L. Tholence and R. Tournier, J. Phys. (Paris) Colloq. 35, C4-229 (1974).

[19]A. P. Murani, Phys. Rev. Lett. 37, 450 (1976).

[20]A. P. Murani, J. Magn. Magn. Mater. 5, 95 (1977).

[21]C. N. Guy, Physica **86-88B**, 877 (1977).

[22]C. N. Guy, J. Phys. F **7**, 1505 (1977).

[23]P. A. Beck, Metall. Trans. **2**, 2015 (1971).

[24]V. Cannella, in *Amorphous Magnetism*, edited by H. O. Hooper and A. M. DeGraaf (Plenum, New York, 1973), p. 195.

[25]S. F. Edwards and P. W. Anderson, J. Phys. F **5**, 965 (1975).

[26]A. A. v. d. Giessen, J. Phys. Chem. Solids **29**, 343 (1967).

[27]K. Zaveta, J. Schneider, A. Handstein, and F. Zounova, in *Rapidly Quenched Metals III*, edited by B. Cantor (The Metals Society, London, 1978), Vol. 2, p. 156.

[28]C. Guillaud, C. R. Acad. Sci. **219**, 614 (1944).

[29]R. Hahn and E. Kneller, Z. Metallkd. **49**, 426 (1958). Note, however, that their modification of the Langevin function to include a distribution in cluster size was for a well-ordered alloy with long-range-ordered clusters.

[30]N. V. Volkenshtein, M. I. Turchinskaya, and E. V. Galoshina, Zh. Eksp. Teor. Fiz. **35**, 1312 (1958) [Sov. Phys. JETP **35**, 916 (1959)].

[31]G. Zibold, J. Phys. F **8**, L229 (1978).

[32]F. Holtzberg, J. L. Tholence, H. Godfrin, and R. Tournier, J. Appl. Phys. **50**, 1717 (1979).

[33]C. A. M. Mulder, A. J. van Duyneveldt, and J. A. Mydosh, Phys. Rev. B **23**, 1384 (1981).

[34]A. K. Mukhopadhyay, R. D. Shull, and P. A. Beck, J. Less-Common Met. **43**, 69 (1975).

[35]E. M. Gray, J. Phys. F **9**, L167 (1979).

[36]E. D. Dahlberg, M. Hardiman, R. Orbach, and J. Souletie, Phys. Rev. Lett. **42**, 401 (1979).

[37]S. Chikazumi, *Physics of Magnetism* (Wiley, New York, 1964), p. 313.

[38]E. P. Wohlfarth, Phys. Lett. **70A**, 489 (1979).

[39]N. V. Volkenshtein, N. I. Kourov, and Yu. N. Tsiovkin, Fiz. Met. Metalloved. **42**, 213 (1976) [Phys. Met. Metallogr. (USSR) **42**, 190 (1976)].

[40]J. S. Kouvel, J. Phys. Chem. Solids **21**, 57 (1961).

[41]T. Taoka, J. Phys. Soc. Jpn. **11**, 537 (1956).

[42]I. S. Jacobs and J. S. Kouvel, Phys. Rev. **122**, 412 (1961).

[43]J. S. Kouvel and C. D. Graham, J. Appl. Phys. **30**, 312S (1959).

[44]T. Satoh, R. B. Goldfarb, and C. E. Patton, Physica **86-88B**, 820 (1977).

[45]W. H. Meiklejohn, Rev. Mod. Phys. **25**, 302 (1953).

[46]E. F. Wassermann and J. L. Tholence, in *Magnetism and Magnetic Materials—1975*, edited by J. J. Becker, G. H. Lander, and J. J. Rhyne, AIP Conf. Proc. No. 29 (AIP, New York, 1976), p. 237.

[47]R. W. Knitter, J. S. Kouvel, and H. Claus, J. Magn. Magn. Mater. **5**, 356 (1977).

[48]J. J. Préjean, J. Phys. (Paris) Colloq. **39**, C6-907 (1978).

[49]H. Maletta, W. Felsch, and J. L. Tholence, J. Magn. Magn. Mater. **9**, 41 (1978).

[50]H. v. Löhneysen and J. L. Tholence, Phys. Rev. B **19**, 5858 (1979).

[51]S. P. McAlister and M. R. Freeman, J. Phys. F **10**, L211 (1980).

[52]F. D. Stacey and S. K. Banerjee, *The Physical Principles of Rock Magentism* (Elsevier, Amsterdam, 1974), p. 106.

[53]E. P. Wohlfarth, J. Phys. F **10**, L241 (1980).

[54]J. S. Kouvel, C. D. Graham, and J. J. Becker, J. Appl. Phys. **29**, 518 (1958).

[55]A. S. Yermolenko and M. I. Turchinskaya, Fiz. Metal. Metalloved. **21**, 305 (1966) [Phys. Met. Metallogr. (USSR) **21**, 156 (1966)].

[56]R. B. Goldfarb, K. V. Rao, F. R. Fickett, and H. S. Chen, J. Appl. Phys. **52**, 1744 (1981).

[57]Y. Obi, H. Morita, and H. Fujimori, Phys. Status Solidi A **55**, K67 (1979).

[58]A. Blanchard and V. Tutovan, C. R. Acad. Sci. **261**, 2852 (1965).

[59]T. Satoh, Y. Yokoyama, and I. Oguro, Bull. Electrotech. Lab. (Tokyo) **34**, 116 (1970).

[60]T. Satoh, Y. Yokoyama, and I. Oguro, J. Magn. Magn. Mater. **5**, 18 (1977).

[61]Y. Murakami, Trans. Jpn. Inst. Met. (Sendai) **16**, 333 (1975).

[62]T. Iwata, K. Kai, T. Nakamichi, and M. Yamamoto, J. Phys. Soc. Jpn. **28**, 582 (1970).

[63]The temperature at which the anitiparallel Mn spins first acquire their viscosity has not been addressed but is possibly near room temperature based on the temperature at which the reversed remanence dissappears after TRM reversal (Ref. 6).

[64]Y. Kitaoka, K. Ueno, and K. Asayama, J. Phys. Soc. Jpn. **44**, 142 (1978).

[65]The effects of the antiparallel spins are stronger in the weakly ordered alloys than in the disordered. This is possibly due to the initial increase with ordering of small clusters ferromagnetically coupled to antiparallel Mn spins.

[66]G. Zibold and D. Korn, J. Magn. Magn. Mater. **15-18**, 143 (1980).

[67]D. R. Rhiger, D. Müller, and P. A. Beck, J. Magn. Magn. Mater. **15-18**, 165 (1980).

[68]P. A. Beck, Solid State Commun. **34**, 581 (1980).

[69]M. Hardiman, Bull. Am. Phys. Soc. Ser. II **25** (3), 176 (1980).

[70]A. P. Murani, Solid State Commun. **33**, 433 (1980).

[71]J. L. Tholence, Solid State Commun. **35**, 113 (1980).

[72]R. Cywinski and E. M. Gray, Phys. Lett. **77A**, 284 (1980).